THE JOURNAL OF PHYSICAL CHEMISTRY C
A JOURNAL OF THE AMERICAN CHEMICAL SOCIETY
pubs.acs.org/JPCC
Article

Oxidation of Gas-Phase and Supported Pt Nanoclusters: An *Ab Initio* Investigation

Mina Taleblou, Matteo Farnesi Camellone, Stefano Fabris, and Simone Piccinin*

Cite This: *J. Phys. Chem. C* 2022, 126, 10880−10888
Read Online
ACCESS | Metrics & More | Article Recommendations | Supporting Information

ABSTRACT: Heterogeneous catalysts based on Pt nanoparticles supported on oxides are used in a number of important catalytic processes, including oxidation of hydrocarbons and redox reactions in PEM fuel cells. The interaction with gas-phase oxygen is often a key component of the target chemistry and can affect the reactivity of the clusters because of their oxidation. Recent experiments have shown that the oxidation of Pt nanoparticles is influenced by a number of factors, including the clusters size and the interaction with the support, leading to properties that can differ substantially from those of larger samples. Here we combine density functional theory, the genetic algorithm, and *ab initio* thermodynamics to investigate the structure and the oxidizability of small Pt_x (x = 1−8) nanoparticles. We find that the interaction of oxygen with Pt depends strongly on the size of the clusters, leading to facile oxidation of Pt nanoparticles. The interaction with the oxide supports studied in this work, brookite TiO_2 and Co_3O_4, hinders the oxidizability compared to the gas phase. At conditions of temperature and pressure typically encountered in catalytic oxidation reactions, Pt nanoparticles are predicted to be oxidized, at variance with the bulk counterpart. Our results highlight the importance of low Pt−Pt coordination in the interaction with oxygen and the role of the interaction with oxide supports.

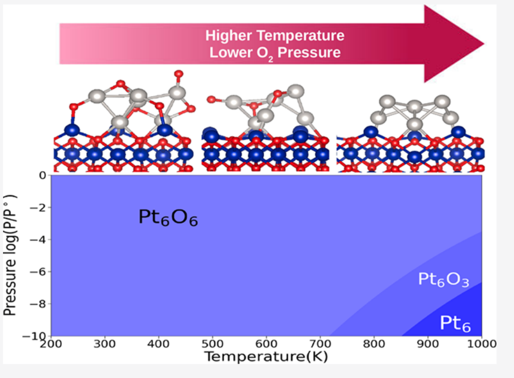

■ INTRODUCTION

Heterogeneous catalysts, often in the form of metal particles supported on oxides, play an important role in many industrial chemical processes and in environmental protection.[1,2] Platinum supported on transition-metal oxides, in particular, is employed to promote a variety of chemical processes, such as oxidation and reduction reactions in proton-exchange membrane fuel cells,[3,4] oxidation of hydrocarbons,[5] and the treatment of exhaust gases.[6,7] The interaction of gas-phase oxygen with bulk Pt has been studied in great detail, both experimentally[8,9] and theoretically.[10,11] Pt, however, is often used in the form of nanoparticles (NPs) to take advantage of their high surface-to-volume ratio and to optimize the use of this rare and expensive element. Similar to bulk Pt, there have been works investigating the oxidation of Pt NPs in catalytic conditions.[12,13] Because the oxidation state of Pt NPs has a strong impact on their catalytic properties,[14,15] it is crucial to understand how different factors such as size of NPs, interaction of NPs with the support, and conditions of the gas-phase atmosphere affect the propensity of Pt NPs to be oxidized. Theoretical studies have shown that the oxidation of Pt NPs in the gas phase is strongly influenced by the size of the clusters.[16,17] Experimental and theoretical studies have shown that the oxidizability of NPs not only is a function of the size of the system, temperature, and pressure of the gas-phase environment but also depends on the nature of metal oxide support.[18−21] Despite the importance of the topic, the role of the support on the oxidation of Pt NPs has not yet been investigated in detail.

One of the challenges in modeling the supported oxidized clusters is the structural complexity of these systems, preventing the use of simple structural optimization approaches and requiring the use of advanced global optimization algorithms. To this end, here we employ the genetic algorithm (GA) coupled with density functional theory (DFT)[22] to explore and predict the most stable structures of metallic and oxidized Pt clusters of different sizes and stoichiometries, both in the gas phase and supported on oxide surfaces. Brookite TiO_2 and Co_3O_4, two reducible metal oxides, are selected as supporting surfaces. We focus on the thermodynamic properties of these systems to predict temperature and pressure conditions for the formation of oxide clusters, trends as a function of the size, and discussing the role of the interaction with the support in oxidation of Pt clusters.

Received: March 30, 2022
Revised: June 14, 2022
Published: June 28, 2022

https://doi.org/10.1021/acs.jpcc.2c02176
J. Phys. Chem. C 2022, 126, 10880−10888

■ COMPUTATIONAL DETAILS

The DFT calculations were performed with the Quantum ESPRESSO code,[23] employing a plane-wave basis set and pseudopotentials. We adopted the Perdew−Burke-Ernzerhof (PBE) approximation for the exchange and correlation functional.[24] To model Co_3O_4, we used the DFT+U approach, adding a Hubbard term on the d states of Co atoms. Following previous works,[25] we used U = 3.0 eV for Co. In the case of stoichiometric TiO_2, we verified that the effect of adding a U = 3.5 eV Hubbard term on the formation energy of Pt oxide clusters is negligible, and we therefore performed a PBE calculation. Whereas in the presence of oxygen vacancies (i.e., reduction of Ti^{4+} to Ti^{3+}) on the brookite surface, the addition of the Hubbard term (U = 3.5 eV) is necessary to calculate the formation energy of oxygen vacancy. We employed ultrasoft pseudopotentials to describe Pt, Ti, and Co ions, while a projector augmented wave pseudopotential was used for oxygen. For all the clusters simulations, k-point sampling of the Brillouin zone was performed at the gamma point and a Marzari−Vanderbilt scheme with a width of 0.136 eV was used to smear the electronic occupations.

To find the structural global minima (GM) of Pt and PtO_x clusters, we used the genetic algorithm (GA) as implemented in Atomic Simulation Environment (ASE) package.[22] This algorithm is applicable in structural optimization of both gas-phase and supported clusters.[26,27] For details regarding the implementation of GA in ASE and its performance, we refer the reader to the original work of Vilhelmsen and Hammer.[22,28] For details regarding the setup of the GA calculations in the present work, we refer the reader to the Supporting Information, where we also report the input files to run GA with ASE in combination with Quantum ESPRESSO on a parallel machine using communication via sockets.

Gas-phase Pt and Pt oxide clusters are simulated in a large 20 × 20 × 20 Å^3 cubic cell. To model the oxidation of Pt clusters, we considered five different stoichiometries, namely, Pt_xO_y clusters with y/x = 0, 0.5, 1, 1.5, and 2, and consider clusters containing up to eight Pt atoms. The search for the GM of gas-phase clusters is performed in three steps: First, the GA algorithm was used in combination with the LAMMPS program to exploit the efficient reactive force field developed for the Pt−O system by Fantauzzi and co-workers.[29] The 20 most stable structures found from this step were then used as initial candidates for GA calculations at DFT level.

To perform the structural relaxation within the GA calculations, we used loose criteria for the plane wave cutoff and forces: The Kohn−Sham orbitals are expanded up to a kinetic energy of 25 Ry for the wave function and 200 Ry for the charge density, and the maximum convergence force criterion for geometry optimization is 0.05 eV/Å per atom. The GM is then further optimized by a more stringent cutoff energy of 50/500 Ry and a force threshold of 0.026 eV/Å.

The cohesive energy of gas-phase metallic clusters, normalized per Pt atom, is calculated as

$$E_{coh} = (E(Pt_x) - E(Pt_{iso}))/x \quad (1)$$

where $E(Pt_x)$is the total energy of the gas-phase cluster, $E(Pt_{iso})$is the total energy of an isolated Pt atom, and x is the number of Pt atoms in the cluster. Using the total energy of Pt atom in the bulk form instead of isolated Pt would result in positive cohesive energy. To investigate the oxidation of metallic clusters, we computed their formation energy (E_{form}), normalized per O atom, defined as

$$E_{form}(Pt_xO_y) = \frac{1}{y}\left(E(Pt_xO_y) - E(Pt_x) - \frac{1}{2}yE(O_2)\right) \quad (2)$$

Here, $E(Pt_xO_y)$ is the total energy of the oxidized cluster, $E(O_2)$is the total energy of the molecular oxygen, and y is the number of oxygen atoms in the system.

Also in the case of supported clusters we adopted a two-step procedure. We first performed GA calculations with a cutoff of 25/200 Ry and a maximum force threshold of 0.05−0.2 eV/Å, depending on the size of the system. We then optimized the most stable structure with the same parameters of gas phase clusters (a cutoff of 50/500 Ry and a force threshold of 0.026 eV/Å).

Periodic slabs of brookite TiO_2(210) and Co_3O_4(111) were modeled by using (1 × 2) and (2 × 2) supercells, respectively. When modeling the TiO_2/Pt_8 and the Co_3O_4/Pt_8 or Co_3O_4/Pt_8O_8 systems, to avoid the interaction between periodic replicas of the clusters, the size of the cells were doubled; that is, we employed (1 × 4) and (2 × 4) supercells, respectively. In all the calculations, the bottom two layers of the slabs were fixed, while the rest of the layers were allowed to relax. To avoid spurious interactions among periodic replicas of the slabs, we included 12 Å of vacuum in the direction normal to the surface. All calculations are spin polarized, with the exception of supported clusters on TiO_2, where we found negligible effects (<0.1 eV) of spin polarization on the formation energy of the supported clusters. To model the TiO_2 (210) surface, we considered a stoichiometric slab, consisting of four Ti layers. To model the polar Co_3O_4(111) surface, we employ a symmetric, nonstoichiometric slab, as done in one of our previous works on this system.[25] Here we use a slab that includes a total of 11 layers, the same model used by Yan and Sautet.[30] In the Supporting Information we display the structural models adopted in our study, for the case of Pt_6 supported on the two oxides.

The adsorption energy of metallic clusters on the TiO_2 and Co_3O_4 surface is calculated as[31]

$$E_{ads} = (E(Pt_x@slab) - E(slab) - E(Pt_x)) \quad (3)$$

Here, $E(Pt_x@slab)$is the total energy of the supported Pt cluster, $E(slab)$is the total energy of the clean surface, and $E(Pt_x)$is the total energy of the metallic cluster where all systems have been relaxed. The formation energy of supported Pt oxide clusters was defined in analogy with gas-phase species.

Additional calculations for bulk platinum, PtO (tetragonal, *P42/mmc*), and β-PtO_2 (orthorhombic, *Pnnm*) were performed as reference by using the primitive unit cells, a 8 × 8 × 8 k-point mesh, and a cutoff of 410 eV. The lattice parameter of optimized bulk Pt was found to be 3.96 Å, overestimated by 1% with respect to the experimental value of 3.92 Å.[32] The structural parameters of PtO (a = 3.14, b = 5.33 Å) and β-PtO_2 (a = 4.43, b = 4.53, c = 3.13 Å) compare favorably with the experimental measurements (a = 3.08, b = 5.34 Å)[33] and (a = 4.48, b = 4.53, c = 3.13 Å)[34] for PtO and β-PtO_2, respectively.

The cohesive energy of Pt bulk system was calculated to be −5.58 eV, in good agreement with the experimental value of −5.85 eV.[35] The calculated heat of formation for bulk PtO and β-PtO_2 with respect to the total energy of bulk Pt and molecular oxygen, is −0.48 eV/Pt and −1.44 eV/Pt, respectively. These values are consistent with previous

https://doi.org/10.1021/acs.jpcc.2c02176
J. Phys. Chem. C 2022, 126, 10880−10888

theoretical works, − 0.68 eV/−1.42 eV[17] and −0.55 eV/−1.57 eV,[10] and are in good agreement with the experimental measurements, −0.71 eV/−1.38 eV.[36] This good agreement happens in spite of the severe overestimation of the binding energy of the oxygen molecule, largely due to the PBE functional (−6.66 eV against the experimental −5.23 eV), which suggests a large error cancellation when computing the heat of formation via eq 2.

Vibrational frequencies were calculated based on a finite difference scheme in which atoms are shifted with 0.01 Å displacement along three dimensions. The contribution of ZPE in the total energy of the clusters is less than 0.05 eV/O for all the systems; hence, it is not included in thermodynamics calculations. To compute atomic charges, we used the Bader partitioning scheme employing Henkelman et al.'s code.[37]

To investigate the thermodynamic stability of both gas phase and supported clusters in an oxidizing atmosphere, we employed the *ab initio* thermodynamics framework.[38] We treated the gas-phase oxygen as an ideal gas, whose chemical potential (μ_O) depends on temperature and pressure according to

$$\mu_O(T, p) = \mu_O(T, p^\circ) + \frac{1}{2}k_BT \ln\left(\frac{p}{p^\circ}\right) \tag{4}$$

where p° is the standard pressure, 1 bar, and k_B is the Boltzmann constant. The temperature dependence of μ_O at p° is obtained from the JANAF thermochemical tables.[39] We define the change in the chemical potential of oxygen relative to its zero-temperature value as

$$\Delta\mu_O(T, p) = \mu_O(T, p) - \frac{1}{2}E(O_2) \tag{5}$$

To compute the Gibbs free energy of formation as a function of the oxygen chemical potential, we write

$$\Delta G(T, p) = G(Pt_xO_y) - G(Pt_x) - y\mu_O(T, p) \tag{6}$$

$$\simeq E(Pt_xO_y) - E(Pt_x) - y\left(\frac{1}{2}E(O_2) + \Delta\mu_O(T, p)\right) \tag{7}$$

$$= yE_{form}(Pt_xO_y) - y\Delta\mu_O(T, p) \tag{8}$$

Here we have approximated the free energy of metal and oxide clusters with their DFT total energy. While this approximation is reasonable for supported clusters, gas-phase clusters have large contributions from translational and rotational entropy, which cannot be ignored. We therefore checked explicitly the effects of such contributions. We found that the entropic contributions in gas-phase clusters do not affect significantly the Gibbs free energy of formation. The reason is that the entropic contribution in metallic and oxidized clusters are quantitatively very similar and enter in eq 8 with an opposite sign. For example, in the case of Pt_4O_8 such effect at 600 K is of the order of 10 meV, which is negligibly small.

RESULTS AND DISCUSSION

Morphological Studies. *Gas-Phase Clusters.* The GA algorithm was applied to search for the most stable structures of Pt and Pt_xO_y clusters in the gas phase. The lowest energy configurations for pure Pt_x clusters (x = 2, 4, 6, 7, 8, and 10) are shown in Figure 1. The computed bond length of the Pt_2 dimer is 2.31 Å. Pt_3 is an equilateral triangle in agreement with previous studies.[17,40,41] Our calculations suggest that the most stable structure for Pt_4 is planar, even though the 3D tetrahedron structure is only 0.1 eV higher in energy. This result is in line with other studies[17,42,43] where the lowest energy Pt_4 structure is found to be either the planar or the 3D one, depending on the details of the calculation, suggesting that these two structures are indeed very close in energy. The calculations show that a 2D to 3D transition occurs from Pt_6 to Pt_7. Pt_6 exhibits a 2D planar triangular structure, whereas Pt_7 has a 3D structure. The structure of Pt_7 has the same planar geometry of Pt_6 with an additional Pt atom at one corner which forms a triangle vertical to the rest planar atoms. A similar structure was predicted for Pt_7 in a recent study.[44]

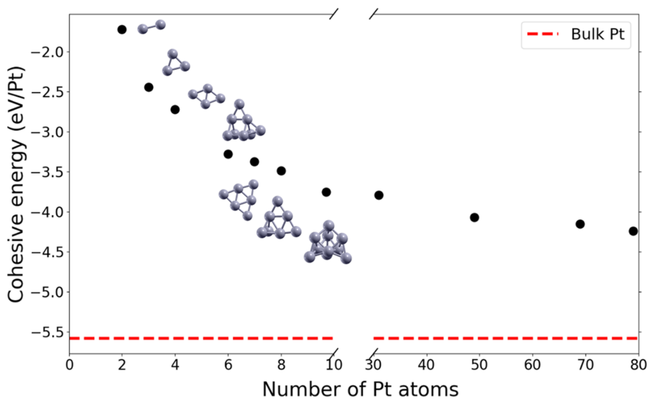

Figure 1. Cohesive energy of gas-phase Pt clusters.

Pt_8 and Pt_{10} clusters exhibit a pyramid-like tetrahedral structure. The computed average Pt−Pt bond length of all the Pt clusters is found to be 2.53 Å. Our morphological studies are comparable with previous theoretical works.[17,45]

Figure 1 shows a plot of the cohesive energy of the gas-phase Pt metallic clusters as a function of the cluster size, computed according to eq 1. We considered also larger Pt NPs, containing 19−79 atoms, to partially bridge the gap between small Pt clusters and Pt bulk. In this case, we did not optimize the NPs by using the GA, but we simply built the structures from bulk coordinates using the NanoCrystal tool[46] and then performed a structural optimization.

Our calculations clearly show that the cohesive energy decreases monotonically with increasing cluster size. As reported by previous studies,[17,40,47] the tendency of larger Pt_x ($x > 6$) clusters to adopt a 3D structure is related to the strong interaction between Pt atoms.

Having investigated the structure and stability of gas-phase Pt clusters, we now focus our attention to the study of the oxidation of Pt metallic clusters. Figure 2 shows the lowest energy configurations of Pt_xO_y clusters. The Pt_2O_y and Pt_4O_y oxide clusters adopt a linear and almost symmetric configuration. Larger Pt oxide clusters, Pt_xO_y ($x \geq 6$), exhibit a ring shape structure, in agreement with previous studies.[17] O atoms of the oxidized clusters, in most of the cases, prefer to bind to two Pt atoms, minimizing the number of O−O bonds. The exceptions are large clusters with the Pt_xO_{2x} stoichiometry (i.e., Pt_6O_{12}, Pt_7O_{14}, and Pt_8O_{16}) where several O−O bonds are present.

The computed formation energies of Pt_xO_x, $Pt_xO_{1.5x}$ and Pt_xO_{2x} clusters are shown in Figure 3 and compared to the PtO and PtO_2 bulk ones (horizontal green and dark green dashed lines, respectively). It is clear form Figure 3 that Pt_xO_y nanoclusters have much lower formation energies than bulk PtO or PtO_2 and that, as the size of the clusters increases, the

https://doi.org/10.1021/acs.jpcc.2c02176
J. Phys. Chem. C 2022, 126, 10880−10888

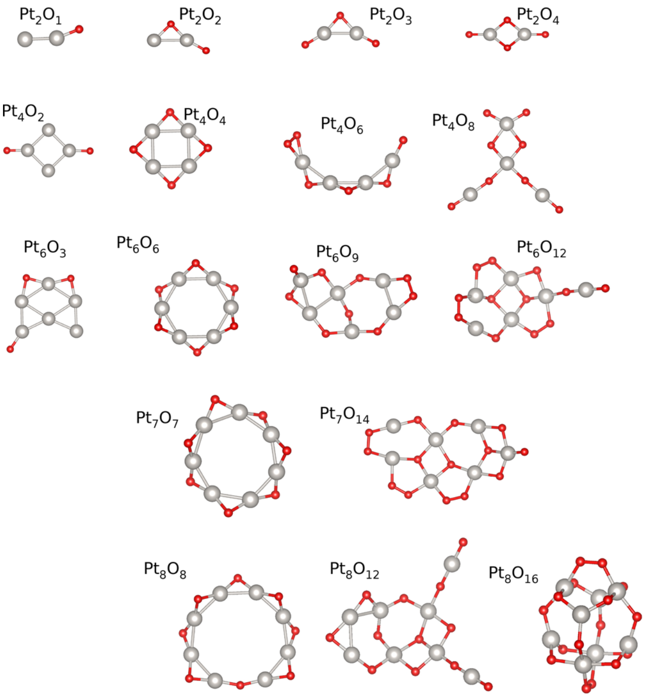

Figure 2. Global minima structures of Pt oxide clusters in the gas phase.

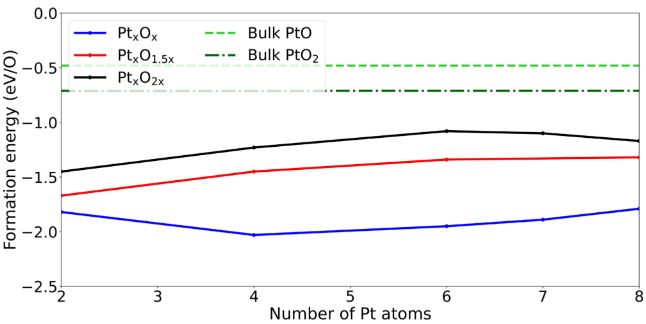

Figure 3. Formation energy of Pt oxide clusters in the gas phase.

formation energy tends to approach the bulk levels, in agreement with the work of Xu et al.[17] The affinity for oxygen is therefore larger for smaller Pt clusters.

Upon comparison of the formation energies of Pt_xO_x and Pt_xO_{2x} clusters, Figure 3 shows that at the DFT level the formation energy of Pt_xO_x is more negative, in line with a previous report.[16] Though, this is the opposite of what happens in the bulk, where the formation energy of PtO_2 is lower than that of PtO.

Comparing the formation energy per oxygen atom of Pt_xO_x and Pt_xO_{2x} clusters, Figure 3 shows that the formation energy of Pt_xO_x is more negative, in line with a previous report.[16] This, however, is the opposite of what happens in the bulk, where the formation energy of PtO_2 is lower than that of PtO.[11] Interestingly, we find that the formation energy of clusters with fractional $Pt_xO_{1.5x}$ stoichiometry has an intermediate value between those of the other two oxides. This suggests that the oxidation of Pt clusters proceeds according to the sequence $Pt_x \rightarrow Pt_xO_x \rightarrow Pt_xO_{1.5x} \rightarrow Pt_xO_{2x}$, while in the bulk the PtO phase is not thermodynamically stable, as already reported in previous works.[11]

Supported Clusters. In this section we focus on the interaction of metallic and oxidized Pt clusters with $Co_3O_4(111)$ and brookite $TiO_2(210)$ surfaces. To this end, as in the case of gas-phase Pt clusters, we employ the GA algorithm to identify low-energy structures of Pt and Pt_xO_y clusters supported on the metal/oxide surfaces (see the Computational Details section). Figure 4 shows the lowest energy structures of Pt metallic and oxidized clusters adsorbed on $Co_3O_4(111)$ and $TiO_2(210)$ surfaces.

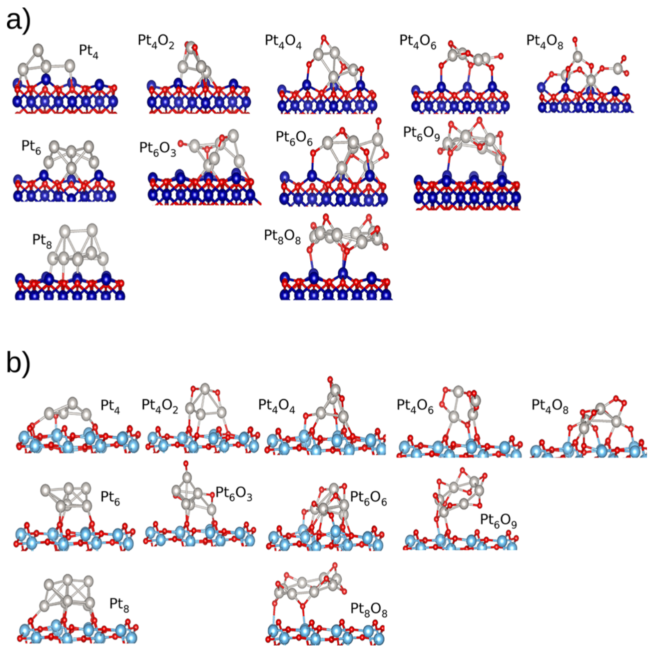

Figure 4. Supported Pt and Pt-oxide clusters on (a) $Co_3O_4(111)$ and (b) $TiO_2(210)$ metal oxide supports. Gray and red spheres represent Pt and O atoms, respectively.

The metallic Pt_4 cluster has an almost planar structure on both supports that is similar to the gas-phase case. Instead, the Pt_6 and Pt_8 metallic clusters adopt a bilayer structure in agreement with a previous theoretical study.[48] This is in contrast with the results reported in an experimental study[49] where it is shown that Pt_4 and Pt_7 metallic clusters supported on a rutile TiO_2 (110) surface are flat and bilayer structures are observed for larger Pt clusters. The oxidized Pt_4O_y clusters exhibit 3D structures when adsorbed on both the supports. When adsorbed on the $TiO_2(210)$ surface, the Pt_6O_6 cluster presents a ringlike shape, similarly to the gas-phase case, whereas it assumes a 3D shape on the $Co_3O_4(111)$ support. On both the supports, the oxidized Pt_6O_9 and Pt_8O_8 clusters have a ringlike structure.

The adsorption energies of the Pt metallic clusters supported on the on $TiO_2(210)$ and $Co_3O_4(111)$ surfaces are reported in Figure 5a as a function of the cluster size. The Pt metallic clusters adsorb more strongly on $Co_3O_4(111)$ compared to $TiO_2(210)$, and the larger the Pt cluster, the stronger the interaction with the support, with the exception of the Pt_1 on $TiO_2(210)$.

In a similar study,[50] Wanbayor and Ruangpornvisuti have shown that the Pt adatom binds strongly on the anatase $TiO_2(001)$ surface (the adsorption energy being −2.6 eV), whereas other metal adatoms such as Au and Pd adsorb more weakly on the same surface (with adsorption energies of −1.51

https://doi.org/10.1021/acs.jpcc.2c02176
J. Phys. Chem. C 2022, 126, 10880−10888

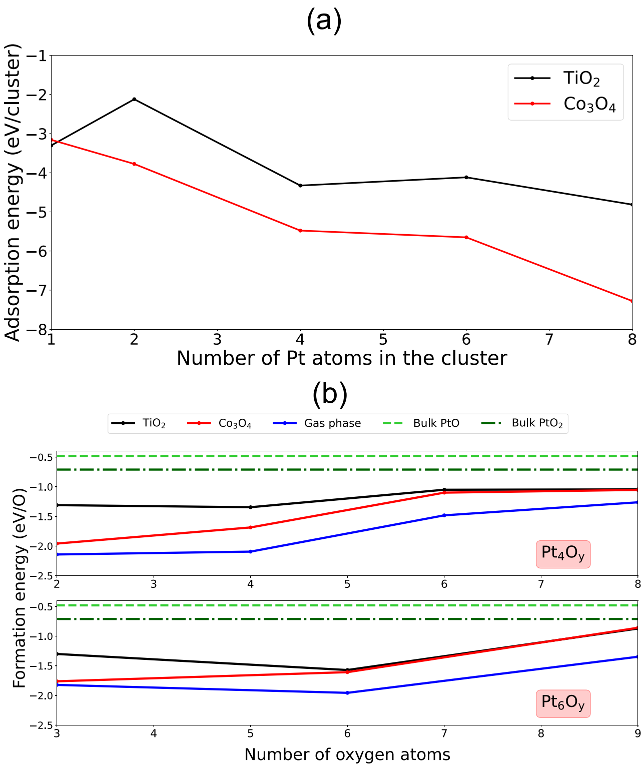

Figure 5. (a) Adsorption energy of supported Pt clusters. (b) Formation energy of Pt_4O_y and Pt_6O_y clusters supported on TiO_2 and Co_3O_4.

and −1.39 eV, respectively). In the work of Wang et al. the computed adsorption energies of a single Pt atom and a dimer Pt_2 on the same anatase $TiO_2(001)$ support are found to be −2.5 and −1.6 eV, respectively.

When considering larger Pt clusters, it has been shown that the adsorption energy (using the total energy of the Pt cluster as reference) of a Pt_5 nanocluster supported on the $Co_3O_4(220)$ surface is −4.75 eV.[51] The corresponding quantities in our study for Pt_4 and Pt_6 on $Co_3O_4(111)$ are −5.47 and −5.65 eV.

Figure 5b shows a plot of the formation energies (FEs) of the supported oxidized Pt_4O_y and Pt_6O_y clusters as a function of the number of O atoms (y). Our calculations show that the formation energies of clusters supported on the $Co_3O_4(111)$ and $TiO_2(210)$ surfaces are higher than those in the gas phase, suggesting that it is easier to oxidize gas-phase Pt clusters with respect to supported Pt clusters. Moreover, the oxidation of supported Pt clusters follows a trend similar to the gas-phase case: Smaller Pt clusters are easier to oxidize compared to larger ones. Interestingly, for Cu clusters a reverse size dependency of oxidation was found upon adsorption on the support:[18] the smaller the clusters, the more difficult it is to oxidize them in the gas phase, while the opposite happens when supported.

A significant finding of this investigation is the comparison displayed in Figure 5b between the formation energy of oxide nanoclusters and bulk phases. For both gas-phase and supported clusters, the FEs are significantly lower (by at least a factor 2) than the corresponding formation energy values of bulk PtO and PtO_2. This indicates that small gas-phase or supported Pt clusters are much easier to oxidize compared to Pt bulk. This finding can help rationalizing the recent experimental evidence of the oxidation of Pt clusters supported on $Co_3O_4(111)$ at conditions of temperature and pressure where oxidation of bulk Pt could be excluded.[52]

Another interesting finding is that the effect of the type of support depend on size, too: The FE of the clusters with a high oxygen content (Pt_4O_6, Pt_4O_8, Pt_6O_6, and Pt_6O_9) is very weakly affected by the type of support, whereas some significant differences can be detected at low oxygen content.

The atoms included in the GA optimization comprise both the atoms of the clusters and the oxygen atoms of the first layer of the support. The lowest energy structures, however, never result in the oxidation of the Pt clusters via the creation of oxygen vacancies. To rationalize this finding, we computed the formation energy of an oxygen vacancy on the pristine brookite surface as well at the interface between the brookite surface and the Pt_6 cluster, obtaining values of 3.52 and 3.14 eV, respectively. The formation energy per oxygen atom of Pt_6O_y, however, is never lower than −2 eV, as shown in Figure 5. This

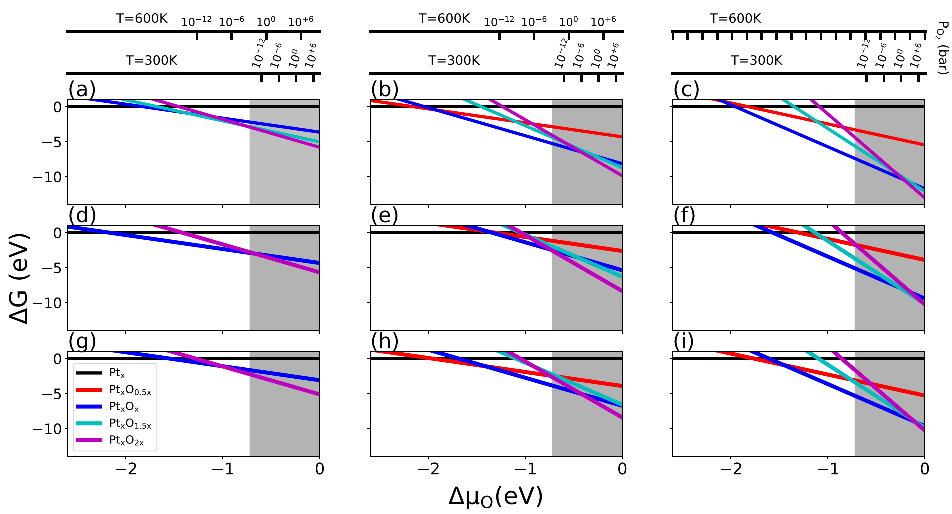

Figure 6. Gibbs free energy of formation of clusters in the gas phase (a−c), supported on TiO_2 (d−f), and supported on Co_3O_4 (g−i). The three panels on the left refer to Pt_2O_x, the three central panels to Pt_4O_x, and the three panels on the right to Pt_6O_x clusters. The shaded area represents the region of stability of bulk β-PtO_2.

https://doi.org/10.1021/acs.jpcc.2c02176
J. Phys. Chem. C 2022, 126, 10880−10888

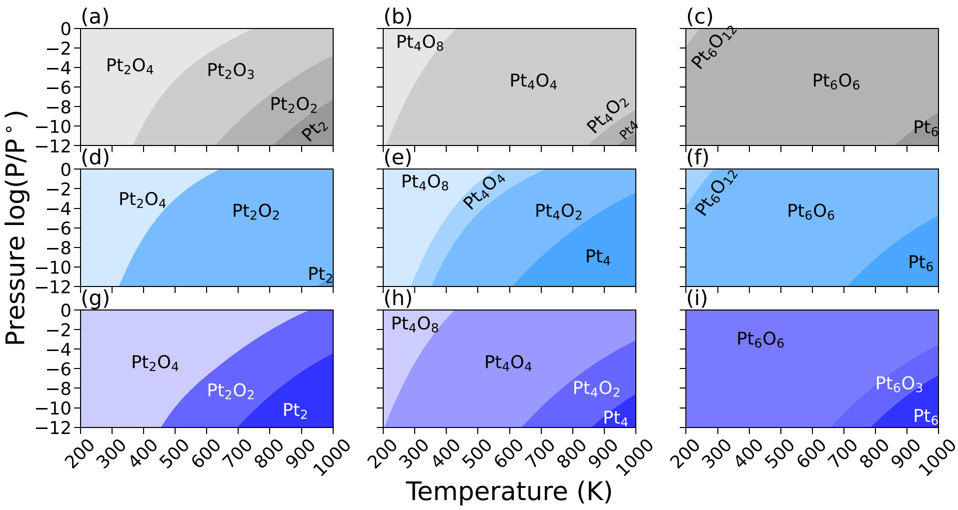

Figure 7. $T-P_{O_2}$ phase diagram of Pt oxide clusters (a−c) in the gas phase (d−f) supported on TiO_2 and (g−i) supported on Co_3O_4.

implies that oxidizing Pt clusters via oxygen from the support is thermodynamically not favorable. Further support for this conclusion comes from a calculation where we created a surface oxygen vacancy in the proximity of the TiO_2/Pt_6 interface and adsorbed the oxygen atom on the Pt_6 cluster. The energy cost with respect to the pristine case is 1.18 eV, in line with the previous estimate. This explains why in the global optimization via the GA we never found structures where the Pt clusters were oxidized via the formation of oxygen vacancies on the support.

***Ab Initio* Thermodynamics.** Let us now focus on the thermodynamic stability of the oxidized Pt clusters both in the gas phase and supported on $Co_3O_4(111)$ and $TiO_2(210)$ surfaces. The phase diagrams showing the Gibbs free energy of formation as a function of the chemical potential of oxygen, $\Delta\mu_O$ (see eq 8), are reported in Figure 6.

Lower values of $\Delta\mu_O$ correspond to more reducing conditions, that is, a lower partial pressure of oxygen and/or higher temperatures (see eqs 4 and 5). For sufficiently low values of $\Delta\mu_O$, the most stable phase of the three clusters sizes examined is the metallic phase, indicated as Pt_x. In all cases, however, this happens at values of $\Delta\mu_O$ lower than −1.5 eV, which are not of practical use: UHV conditions, 10^{-12} bar, correspond to $\Delta\mu_O$ = −0.62 eV at room temperature and −1.32 eV at 600 K.

As the chemical potential of oxygen is increased, oxidized forms of the clusters become thermodynamically stable, with an increasing fraction of oxygen as $\Delta\mu_O$ increases. The transition to the Pt_xO_{2x} stoichiometry takes place in all cases at negative values of $\Delta\mu_O$, suggesting that at ambient conditions (1 bar and room temperature, corresponding to $\Delta\mu_O$ = −0.27 eV) the clusters can be fully oxidized.

Comparing clusters of different sizes, we can see that the transition to the fully oxidized form, Pt_xO_{2x}, requires higher values of $\Delta\mu_O$ for larger clusters. This is consistent with the results displayed in Figure 3 because the affinity for oxygen is larger for smaller clusters. Furthermore, the range of stability of the Pt_xO_x stoichiometry grows for larger clusters.

Comparing gas-phase to supported clusters, we can see that the trends are in all cases similar. The largest difference can be seen for the Pt_6 case, where the formation energy per oxygen atom is considerably lower in the gas phase compared to the supported clusters. Upon comparison of the two supports, TiO_2 and Co_3O_4, the differences are minor. These findings are just another representation of the same effects already highlighted in the previous section when discussing the FE in Figure 5.

An interesting finding is that the range of stability of both the $Pt_xO_{0.5x}$ and $Pt_xO_{1.5x}$ phases is considerably smaller than the Pt_xO_x and Pt_xO_{2x} phases. This is evident also in Figure 7, where we show the stable phases as a function of temperature and pressure for the same nine systems discussed in Figure 6. From these phase diagrams, we predict that both at room temperature and at 600 K Pt nanoclusters are oxidized in the full range of pressures examined, down to UHV conditions. For Pt_2 and Pt_4, the Pt_xO_{2x} phase prevails at room temperature, while the Pt_xO_x phase dominates at 600 K. For the larger Pt_6, on the other hand, only the Pt_xO_x phase appears in the 300−600 K temperature range. The metallic phase of Pt nanoclusters is thermodynamically stable only at very reducing conditions. In UHV the transition of Pt_6O_x clusters to the metallic phase takes place around 900 K in the gas phase and around 700 K on TiO_2.

Similar phase diagrams have been reported by Xu et al. for the gas-phase and stationary small Pt nanoclusters (Pt_x, x = 1, 2, and 3), whose findings agree with the ones reported here.[16] Nair et al. reported a similar oxidation trend for Pt_7.[44]

Our predictions compare favorably with experiments on these systems. Ono and co-workers[54] reported the reduction of PtO_2 NPs supported on TiO_2 to metallic Pt above 550 K in UHV, while some of the Pt NPs supported on SiO_2 remained oxidized up to 750 K in UHV. The same authors also observed a higher temperature for oxygen desorption on NPs compared to Pt(111) and a higher oxygen desorption temperature for smaller nanoparticles compared to larger ones.[53] Moreover, the formation of interfacial PtO_x was observed on Pt NPs at temperatures higher than 400 K for low oxygen pressure (10^{-6} bar) on Co_3O_4.[52]

On the basis of the above discussion, at industrially relevant conditions for catalytic oxidation ($T \sim$ 300−600 K, $P_{O_2} \sim$ 0.1−1 bar), we predict supported nanoclusters to be in an oxidized state, on both supports studied in this work. Small clusters such as Pt_2O_x are found in a fully oxidized state (i.e., Pt^{4+}). As the size of the clusters increases, Pt clusters are predicted to be in both Pt^{4+} and Pt^{2+} oxidation states (higher oxidation state at lower temperatures). As for the largest clusters (Pt_6O_x), these

https://doi.org/10.1021/acs.jpcc.2c02176
J. Phys. Chem. C 2022, 126, 10880−10888

Table 1. Average Positive Bader Charge for Each Pt Atom and Total Magnetization (Number of Up Minus Down Electrons) of Gas-Phase Clusters

Pt_xO_y	spin	Δq (e)	Pt_xO_y	spin	Δq (e)	Pt_xO_y	spin	Δq (e)
Pt_2O_2	0	+0.59	Pt_4O_6	0	+0.77	Pt_7O_7	0	+0.68
Pt_2O_3	0	+0.64	Pt_4O_8	0	+1.22	Pt_7O_{14}	2	+1.05
Pt_2O_4	0	+0.88	Pt_6O_6	0	+0.69	Pt_8O_8	0	+0.69
Pt_4O_2	2	+0.56	Pt_6O_9	0	+0.89	Pt_8O_{12}	1	+0.70
Pt_4O_4	0	+0.69	Pt_6O_{12}	0	+0.98	Pt_8O_{16}	0	+1.17

are mostly found in the Pt^{2+} oxidation state only, indicating an effect of the size on the oxidation state.

Even though in the present work we assumed the system to be in contact with an atmosphere containing only oxygen, in realistic conditions water can also be present and can adsorb and dissociate on the oxide surfaces. In the case of the Co_3O_4 (111) surface, considering oxygen chemical potentials down to −0.5 eV, the surface is partially hydroxylated even in ultrahigh-vacuum (UHV) conditions at 423 K.[30] The hydroxylation of the brookite TiO_2(210) surface has been investigated in a recent work.[55] While surface hydroxylation can have significant effects on the structural and catalytic properties of supported clusters, we did not investigate these effects in the present work.

Charge Transfer. The Bader analysis has been employed to investigate the charge rearrangement at the Pt clusters/oxide interface. First, we have computed the Bader charge of Pt and O atoms of the Pt oxide nanoclusters in the gas phase. This analysis shows that the amount of charge transferred from Pt to O atoms within the clusters varies from +0.5 to +1.2 e per Pt atom. To help assigning the oxidation states, we computed the difference between the Bader charge of Pt bulk (Pt^0) and the Bader charges in bulk Pt^{2+} and Pt^{4+} oxides (Δq). In PtO (Pt^{2+}), Δq on Pt is 0.99 e, in α-PtO_2 (Pt^{4+}) 1.69 e, in β-PtO_2 (Pt^{4+}) 1.73 e, and in β'-PtO_2 (Pt^{4+}) 1.81 e. The fingerprint for the Pt^{2+} oxidation state is therefore a value of Δq around 1 e, while for Pt^{4+} it is 1.7−1.8 e. It is clear from Table 1 that for clusters with a fixed number of Pt_x atoms (x = 2, 4, and 6) Δq, and thus the oxidation state of Pt, increases with increasing the number of O atoms. Because Δq assumes values in between 0.56 and 1.22 per Pt atom, Pt atoms never reach the formal oxidation state of Pt^{4+} found in bulk of PtO_2 oxides. These values for the Bader charges are in agreement with previous studies where some of the same clusters have been considered.[20]

Let us now focus on the interaction between the Pt clusters and the Co_3O_4 and TiO_2 supports. The Bader analysis shows that the binding of the clusters on both supports lead to small charge rearrangements at the Pt cluster/oxides interface (maximum +0.07 e/Pt on TiO_2 and −0.23 e/Pt on Co_3O_4). Therefore, the values of Δq of the Pt atoms of the supported clusters follow a trend similar to the one observed in the gas-phase case.

As an example, we have considered the case of the metallic Pt_4 cluster adsorbed on the Co_3O_4 and TiO_2 oxides (see Figure 8). Also in this case a small amount of charge is transferred from the metallic cluster to the supports. Here, the values of Δq per Pt atom are 0.16 and 0.04 e in the case of Co_3O_4 and TiO_2, respectively. Similar trends have been reported in previous studies: Ammal and co-workers reported Bader charge differences of +0.1 e/Pt for a Pt_3 cluster supported on rutile TiO_2;[56] the same behavior has also been observed for a Pt_5 cluster on the Co_3O_4(220) surface.[51] Our results therefore suggest that the supports have little influence on the electronic properties of the supported metallic and oxidized Pt clusters. Similar small charge transfer was predicted on TiO_2(110) for Ag single atoms.[57] In the Supporting Information we also provide an analysis of the electronic structure of gas-phase and supported clusters based on the d-band model.[58−60]

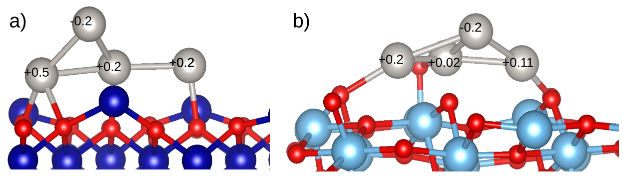

Figure 8. Charge distribution on Pt_4 cluster adsorbed on (a) Co_3O_4 and (b) TiO_2.

■ CONCLUSIONS

In this work we have combined genetic algorithm optimizations with DFT calculations to investigate the structural and thermodynamic properties of Pt nanoparticles, both in the gas phase and supported on oxide surfaces. We considered the interaction of Pt nanoparticles with an oxygen atmosphere, exploring how the size of the clusters and the interaction with the support influence their oxidizability. We found that size has a huge effect on the formation energy of the oxide nanoparticles. The interaction of oxygen with small clusters is much stronger compared to bulk samples, suggesting that nanoparticles can be oxidized at conditions where large samples would still be metallic.

We also found that the interaction with the support hinders, to some extent, the oxidation process compared to gas-phase particles. In spite of this, we predict that at conditions where several catalytic oxidation processes take place (300−600 K, p_{O_2} 0.1−1 bar) Pt nanoparticles are in fact oxidized. Moreover, the tendency of the interaction with oxygen to be stronger for smaller nanoparticles is preserved upon adsorption on oxide surfaces.

The interaction with the two supports examined, brookite TiO_2(210) and Co_3O_4(111), leads to a fairly small charge transfer between the clusters and the support, indicating that the electronic properties of the nanoparticles are not strongly affected by the interaction with the support. Wu and co-workers reported a size-dependent charge transfer between Pt systems and rutile surface, while Pt nanoparticles (1∼2 nm) showed considerable interaction with the support; subnanometer Pt clusters (<1 nm) did not interact with the surface.[61]

■ ASSOCIATED CONTENT

Supporting Information

The Supporting Information is available free of charge at https://pubs.acs.org/doi/10.1021/acs.jpcc.2c02176.

https://doi.org/10.1021/acs.jpcc.2c02176
J. Phys. Chem. C 2022, 126, 10880−10888

GA scripts, optimized structure of both supports with the Pt_6 cluster adsorbed on the surface, calculated d-band center of Pt clusters (PDF)

AUTHOR INFORMATION

Corresponding Author

Simone Piccinin − *CNR-IOM, Consiglio Nazionale delle Ricerche, Istituto Officina dei Materiali, 34136 Trieste, Italy;* orcid.org/0000-0002-3601-7141; Email: piccinin@iom.cnr.it

Authors

Mina Taleblou − *CNR-IOM, Consiglio Nazionale delle Ricerche, Istituto Officina dei Materiali, 34136 Trieste, Italy;* orcid.org/0000-0003-2434-461X

Matteo Farnesi Camellone − *CNR-IOM, Consiglio Nazionale delle Ricerche, Istituto Officina dei Materiali, 34136 Trieste, Italy;* orcid.org/0000-0001-9180-0115

Stefano Fabris − *CNR-IOM, Consiglio Nazionale delle Ricerche, Istituto Officina dei Materiali, 34136 Trieste, Italy;* orcid.org/0000-0003-2562-8788

Complete contact information is available at: https://pubs.acs.org/10.1021/acs.jpcc.2c02176

Notes

The authors declare no competing financial interest.
The Cartesian coordinates of the global minima of all Pt clusters are provided at 10.5281/zenodo.6638351.

REFERENCES

(1) Tran, N.-D.; Farnesi Camellone, M.; Fabris, S. Probing the Reactivity of Pt/Ceria Nanocatalysts toward Methanol Oxidation: From Ionic Single-Atom Sites to Metallic Nanoparticles. *J. Phys. Chem. C* **2018**, *122*, 17917−17927.

(2) Liu, L.; Corma, A. Metal Catalysts for Heterogeneous Catalysis: From Single Atoms to Nanoclusters and Nanoparticles. *Chem. Rev.* **2018**, *118*, 4981−5079.

(3) Vielstich, W., Lamm, A., Gasteiger, H., Eds.; *Handbook of Fuel Cells. Fundamentals, Technology, Applications*; Wiley: West Sussex, 2003.

(4) Farnesi Camellone, M.; Negreiros Ribeiro, F.; Szabová, L.; Tateyama, Y.; Fabris, S. Catalytic Proton Dynamics at the Water/Solid Interface of Ceria-Supported Pt Clusters. *J. Am. Chem. Soc.* **2016**, *138*, 11560−11567.

(5) Marei, M. N.; Khan, H. A.; Badra, J. A.; Montoya, A.; Farooq, A.; Masri, A. R. Comparative Study of the Catalytic Oxidation of Hydrocarbons on Platinum and Palladium Wires and Nanoparticles. *Energy Fuels* **2022**, *36*, 2044−2057.

(6) Kašpar, J.; Fornasiero, P.; Hickey, N. Automotive Catalytic Converters: Current Status and some Perspectives. *Catal. Today.* **2003**, *77*, 419−449.

(7) Kopelent, R.; Tereshchenko, A.; Guda, A.; Smolentsev, G.; Artiglia, L.; Sushkevich, V. L.; Bugaev, A.; Sadykov, I. I.; Baidya, T.; Bodnarchuk, M.; van Bokhoven, J. A.; Nachtegaal, M.; Safonova, O. V. Enhanced Reducibility of the Ceria-Tin Oxide Solid Solution Modifies the CO Oxidation Mechanism at the Platinum-Oxide Interface. *ACS Catal.* **2021**, *11*, 9435−9449.

(8) Mom, R.; Frevel, L.; Velasco-Vélez, J.-J.; Plodinec, M.; Knop-Gericke, A.; Schlögl, R. The Oxidation of Platinum under Wet Conditions Observed by Electrochemical X-ray Photoelectron Spectroscopy. *J. Am. Chem. Soc.* **2019**, *141*, 6537−6544.

(9) van Spronsen, M. A.; Frenken, J. W. M.; Groot, I. M. N. Observing the Oxidation of Platinum. *Nat. Commun.* **2017**, *8*, 429.

(10) Nomiyama, R. K.; Piotrowski, M. J.; Da Silva, J. L. F. Bulk structures of PtO and PtO_2 from Density Functional Calculations. *Phys. Rev. B* **2011**, *84*, 100101.

(11) Seriani, N.; Jin, Z.; Pompe, W.; Ciacchi, L. C. Density Functional Theory study of Platinum Oxides: From Infinite Crystals to Nanoscopic Particles. *Phys. Rev. B* **2007**, *76*, 155421.

(12) Yu, X.; Wang, Y.; Kim, A.; Kim, Y. K. Observation of Temperature-dependent Kinetics for Catalytic CO Oxidation over TiO_2-supported Pt Catalysts. *Chem. Phys. Lett.* **2017**, *685*, 282−287.

(13) Yoshida, H.; Omote, H.; Takeda, S. Oxidation and reduction processes of platinum nanoparticles observed at the atomic scale by environmental transmission electron microscopy. *Nanoscale* **2014**, *6*, 13113−13118.

(14) Zhang, L.; Cheng, X.; Zhang, G.; Qiu, W.; He, H.; Chen, G. High Active Platinum Clusters on Titanium Dioxide Supports toward Carbon Monoxide Oxidation. *Appl. Catal. B* **2020**, *266*, 118629.

(15) Ke, J.; Zhu, W.; Jiang, Y.; Si, R.; Wang, Y.-J.; Li, S.-C.; Jin, C.; Liu, H.; Song, W.-G.; Yan, C.-H.; Zhang, Y.-W. Strong Local Coordination Structure Effects on Subnanometer PtO_x Clusters over CeO_2 Nanowires Probed by Low-Temperature CO Oxidation. *ACS Catal.* **2015**, *5*, 5164−5173.

(16) Xu, Y.; Shelton, W. A.; Schneider, W. F. Thermodynamic Equilibrium Compositions, Structures, and Reaction Energies of Pt_xO_y (x = 13) Clusters Predicted from First Principles. *J. Phys. Chem. B* **2006**, *110*, 16591−16599.

(17) Xu, Y.; Shelton, W. A.; Schneider, W. F. Effect of Particle Size on the Oxidizability of Platinum Clusters. *J. Phys. Chem. A* **2006**, *110*, 5839−5846.

(18) Mammen, N.; Spanu, L.; Tyo, E. C.; Yang, B.; Halder, A.; Seifert, S.; Pellin, M. J.; Vajda, S.; Narasimhan, S. Reversing Size-Dependent Trends in the Oxidation of Copper Clusters through Support Effects. *Eur. J. Inorg. Chem.* **2018**, *2018*, 16−22.

(19) Maurer, F.; Jelic, J.; Wang, J.; Gänzler, A.; Dolcet, P.; Wöll, C.; Wang, Y.; Studt, F.; Casapu, M.; Grunwaldt, J.-D. Tracking the Formation, Fate and Consequence for Catalytic Activity of Pt Single Sites on CeO_2. *Nat. Catal.* **2020**, *3*, 824−833.

(20) Xu, Y.; Getman, R. B.; Shelton, W. A.; Schneider, W. F. A First-Principles Investigation of the Effect of Pt Cluster Size on CO and NO Oxidation Intermediates and Energetics. *Phys. Chem. Chem. Phys.* **2008**, *10*, 6009.

(21) Tovt, A.; Bagolini, L.; Dvořák, F.; Tran, N.-D.; Vorokhta, M.; Beranová, K.; Johánek, V.; Farnesi Camellone, M.; Skála, T.; Matolínová, I.; Mysliveček, J.; Fabris, S.; Matolín, V. Ultimate Dispersion of Metallic and Ionic Platinum on Ceria. *J. Mater. Chem. A* **2019**, *7*, 13019−13028.

(22) Vilhelmsen, L. B.; Hammer, B. A Genetic Algorithm for First Principles Global Structure Optimization of Supported Nano Structures. *J. Chem. Phys.* **2014**, *141*, 044711.

(23) Giannozzi, P.; et al. QUANTUM ESPRESSO: a Modular and Open-source Software Project for Quantum Simulations of Materials. *J. Phys.: Condens. Matter* **2009**, *21*, 395502.

(24) Perdew, J. P.; Burke, K.; Ernzerhof, M. Generalized Gradient Approximation Made Simple. *Phys. Rev. Lett.* **1996**, *77*, 3865−3868.

(25) Lykhach, Y.; Piccinin, S.; Skála, T.; Bertram, M.; Tsud, N.; Brummel, O.; Farnesi Camellone, M.; Beranová, K.; Neitzel, A.; Fabris, S.; Prince, K. C.; Matolín, V.; Libuda, J. Quantitative Analysis of the Oxidation State of Cobalt Oxides by Resonant Photoemission Spectroscopy. *J. Phys. Chem. Lett.* **2019**, *10*, 6129−6136.

(26) Vilhelmsen, L. B.; Hammer, B. Systematic Study of Au_6 to Au_{12} Gold Clusters on MgO(100) F Centers Using Density-Functional Theory. *Phys. Rev. Lett.* **2012**, *108*, 126101.

(27) Rieboldt, F.; Vilhelmsen, L. B.; Koust, S.; Lauritsen, J. V.; Helveg, S.; Lammich, L.; Besenbacher, F.; Hammer, B.; Wendt, S. Nucleation and Growth of Pt Nanoparticles on Reduced and Oxidized Rutile TiO_2 (110). *J. Chem. Phys.* **2014**, *141*, 214702.

(28) Larsen, A. H.; Mortensen, J. J.; Blomqvist, J.; Castelli, I. E.; Christensen, R.; Dulak, M.; Friis, J.; Groves, M. N.; Hammer, B.; Hargus, C.; et al. The Atomic Simulation Environment−a Python Library for working with Atoms. *J. Phys.: Condens. Matter* **2017**, *29*, 273002.

(29) Fantauzzi, D.; Bandlow, J.; Sabo, L.; Mueller, J. E.; van Duin, A. C. T.; Jacob, T. Development of a ReaxFF Potential for Pt-O Systems

describing the Energetics and Dynamics of Pt-oxide Formation. *Phys. Chem. Chem. Phys.* **2014**, *16*, 23118−23133.
(30) Yan, G.; Sautet, P. Surface Structure of Co_3O_4 (111) under Reactive Gas-Phase Environments. *ACS Catal.* **2019**, *9*, 6380−6392.
(31) Nguyen, M.-T.; Farnesi Camellone, M.; Gebauer, R. On the Electronic, Structural, and Thermodynamic Properties of Au Supported on α−Fe_2O_3 Surfaces and their Interaction with CO. *Chem. Phys.* **2015**, *143*, 034704.
(32) Ashcroft, N. W.; Mermin, N. D. *Solid State Physics*; Holt-Saunders: 1976.
(33) McBride, J. R.; Graham, G. W.; Peters, C. R.; Weber, W. H. Growth and Characterization of Reactively Sputtered Thin-film Platinum Oxides. *Int. J. Appl. Phys.* **1991**, *69*, 1596−1604.
(34) Range, K.-J.; Rau, F.; Klement, U.; Heyns, A. β-PtO_2: High Pressure Synthesis of Single Crystals and Structure Refinement. *Mater. Res. Bull.* **1987**, *22*, 1541−1547.
(35) Kittel, C. *Introduction to Solid State Physics*, 8th ed.; Wiley: 2004.
(36) Ono, L. K.; Yuan, B.; Heinrich, H.; Cuenya, B. R. Formation and Thermal Stability of Platinum Oxides on Size-Selected Platinum Nanoparticles: Support Effects. *J. Phys. Chem. C* **2010**, *114*, 22119−22133.
(37) Henkelman, G.; Arnaldsson, A.; Jónsson, H. A Fast and Robust Algorithm for Bader Decomposition of Charge Density. *Comput. Mater. Sci.* **2006**, *36*, 354−360.
(38) Reuter, K.; Scheffler, M. Composition, Structure, and Stability of RuO_2(110) as a Function of Oxygen Pressure. *Phys. Rev. B* **2001**, *65*, 035406.
(39) Allison, T. C. *NIST-JANAF Thermochemical Tables - SRD 13*; 2013.
(40) Majumdar, D.; Dai, D.; Balasubramanian, K. Theoretical Study of the Electronic States of Platinum Trimer (Pt_3). *Chem. Phys.* **2000**, *113*, 7919−7927.
(41) Sebetci, A.; Güvenç, Z. B. Energetics and Structures of Small Clusters: Pt_N, N = 2−21. *Surf. Sci.* **2003**, *525*, 66−84.
(42) Paz-Borbón, L. O.; López-Martínez, A.; Garzón, I. L.; Posada-Amarillas, A.; Grönbeck, H. 2D-3D Structural Transition in Sub-nanometer Pt_N Clusters Supported on CeO_2(111). *Phys. Chem. Chem. Phys.* **2017**, *19*, 17845−17855.
(43) Xiao, L.; Wang, L. Structures of Platinum Clusters: Planar or Spherical? *J. Phys. Chem. A* **2004**, *108*, 8605−8614.
(44) Nair, A. S.; Anoop, A.; Ahuja, R.; Pathak, B. Relativistic Effects in Platinum Nanocluster Catalysis: A Statistical Ensemble-Based Analysis. *J. Phys. Chem. A* **2022**, *126*, 1345−1359.
(45) Kerpal, C.; Harding, D. J.; Hermes, A. C.; Meijer, G.; Mackenzie, S. R.; Fielicke, A. Structures of Platinum Oxide Clusters in the Gas Phase. *J. Phys. Chem. A* **2013**, *117*, 1233−1239.
(46) Chatzigoulas, A.; Karathanou, K.; Dellis, D.; Cournia, Z. NanoCrystal: AWeb-Based Crystallographic Tool for the Construction of Nanoparticles Based on Their Crystal Habit. *J. Chem. Inf. Model.* **2018**, *58*, 2380−2386.
(47) Han, Y.; Liu, C.-j.; Ge, Q. Interaction of Pt Clusters with the Anatase TiO_2(101) Surface: A First Principles Study. *J. Phys. Chem. B* **2006**, *110*, 7463−7472.
(48) Jiang, D.-e.; Overbury, S. H.; Dai, S. Structures and Energetics of Pt Clusters on TiO_2: Interplay between Metal-Metal Bonds and Metal-Oxygen Bonds. *J. Phys. Chem. C* **2012**, *116*, 21880−21885.
(49) Watanabe, Y.; Wu, X.; Hirata, H.; Isomura, N. Size-Dependent Catalytic Activity and Geometries of Size-selected Pt Clusters on TiO_2(110) Surfaces. *Catal. Sci. Technol.* **2011**, *1*, 1490−1495.
(50) Wanbayor, R.; Ruangpornvisuti, V. A periodic DFT Study on Binding of Pd, Pt and Au on the Anatase TiO_2(001) Surface and Adsorption of CO on the TiO_2 Surface-Supported Pd, Pt and Au. *Appl. Surf. Sci.* **2012**, *258*, 3298−3301.
(51) Jana, R.; Chowdhury, C.; Malik, S.; Datta, A. Pt/Co_3O_4 Surpasses Benchmark Pt/C: An Approach Toward Next Generation Hydrogen Evolution Electrocatalyst. *ACS Appl. Energy Mater.* **2019**, *2*, 5613−5621.
(52) Lykhach, Y.; Faisal, F.; Skála, T.; Neitzel, A.; Tsud, N.; Vorokhta, M.; Dvořák, F.; Beranová, K.; Kosto, Y.; Prince, K. C.; Matolín, V.; Libuda, J. Interplay Between the Metal-Support Interaction and Stability in Pt/Co_3O_4(111) Model Catalysts. *J. Mater. Chem. A* **2018**, *6*, 23078−23086.
(53) Ono, L. K.; Croy, J. R.; Heinrich, H.; Roldan Cuenya, B. Oxygen Chemisorption, Formation, and Thermal Stability of Pt Oxides on Pt Nanoparticles Supported on SiO_2 /Si(001): Size Effects. *J. Phys. Chem. C* **2011**, *115*, 16856−16866.
(54) Ono, L. K.; Yuan, B.; Heinrich, H.; Cuenya, B. R. Formation and Thermal Stability of Platinum Oxides on Size-Selected Platinum Nanoparticles: Support Effects. *J. Phys. Chem. C* **2010**, *114*, 22119−22133.
(55) Holmström, E.; Ghan, S.; Asakawa, H.; Fujita, Y.; Fukuma, T.; Kamimura, S.; Ohno, T.; Foster, A. S. Hydration Structure of Brookite TiO_2 (210). *J. Phys. Chem. C* **2017**, *121*, 20790−20801.
(56) Ammal, S. C.; Heyden, A. Modeling the Noble Metal/TiO_2 (110) Interface with Hybrid DFT Functionals: A Periodic Electrostatic Embedded Cluster Model Study. *J. Chem. Phys.* **2010**, *133*, 164703.
(57) Hansen, J.; Lira, E.; Galliker, P.; Wang, J.-G.; Sprunger, P. T.; Li, Z.; Laegsgaard, E.; Wendt, S.; Hammer, B.; Besenbacher, F. Enhanced Bonding of Silver Nanoparticles on Oxidized TiO_2 (110). *J. Phys. Chem. C* **2010**, *114*, 16964−16972.
(58) Hammer, B.; Nørskov, J. Electronic factors determining the reactivity of metal surfaces. *Surf. Sci.* **1995**, *343*, 211−220.
(59) Hammer, B.; Norskov, J. K. Why gold is the noblest of all the metals. *Nature* **1995**, *376*, 238−240.
(60) Hammer, B.; Nørskov, J. *Impact of Surface Science on Catalysis*; Advances in Catalysis; Academic Press: 2000; Vol. *45*, pp 71−129.
(61) Wu, Z.; Li, Y.; Huang, W. Size-Dependent Pt-TiO_2 Strong Metal-Support Interaction. *J. Phys. Chem. Lett.* **2020**, *11*, 4603−4607.